JACS
JOURNAL OF THE AMERICAN CHEMICAL SOCIETY

Article

pubs.acs.org/JACS

Using Dynamic Covalent Chemistry To Drive Morphological Transitions: Controlled Release of Encapsulated Nanoparticles from Block Copolymer Vesicles

Renhua Deng,* Matthew J. Derry, Charlotte J. Mable, Yin Ning, and Steven P. Armes*

Dainton Building, Department of Chemistry, The University of Sheffield, Brook Hill, Sheffield, South Yorkshire S3 7HF, United Kingdom

Supporting Information

ABSTRACT: Dynamic covalent chemistry is exploited to drive morphological order−order transitions to achieve the controlled release of a model payload (e.g., silica nanoparticles) encapsulated within block copolymer vesicles. More specifically, poly(glycerol monomethacrylate)−poly(2-hydroxypropyl methacrylate) (PGMA−PHPMA) diblock copolymer vesicles were prepared via aqueous polymerization-induced self-assembly in either the presence or absence of silica nanoparticles. Addition of 3-aminophenylboronic acid (APBA) to such vesicles results in specific binding of this reagent to some of the pendent cis-diol groups on the hydrophilic PGMA chains to form phenylboronate ester bonds in mildly alkaline aqueous solution (pH ∼ 10). This leads to a subtle increase in the effective volume fraction of this stabilizer block, which in turn causes a reduction in the packing parameter and hence induces a vesicle-to-worm (or vesicle-to-sphere) morphological transition. The evolution in copolymer morphology (and the associated sol−gel transitions) was monitored using dynamic light scattering, transmission electron microscopy, oscillatory rheology, and small-angle X-ray scattering. In contrast to the literature, in situ release of encapsulated silica nanoparticles is achieved via vesicle dissociation at room temperature; moreover, the rate of release can be fine-tuned by varying the solution pH and/or the APBA concentration. Furthermore, this strategy also works (i) for relatively thick-walled vesicles that do not normally exhibit stimulus-responsive behavior and (ii) in the presence of added salt. This novel molecular recognition strategy to trigger morphological transitions via dynamic covalent chemistry offers considerable scope for the design of new stimulus-responsive copolymer vesicles (and hydrogels) for targeted delivery and controlled release of cargoes. In particular, the conditions used in this new approach are relevant to liquid laundry formulations, whereby enzymes require protection to prevent their deactivation by bleach.

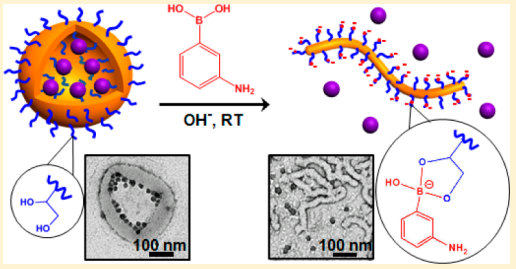

INTRODUCTION

Stimulus-responsive vesicles consisting of polymers, lipids, etc. are excellent candidates for use as smart carriers and nanoreactors.[1−18] It is well-known that amphiphilic diblock copolymers with an appropriate hydrophilic−hydrophobic balance can self-assemble into vesicles (a.k.a. polymersomes) in aqueous solution.[19−24] Various types of functional diblock copolymers can be synthesized with defined composition and controllable molecular weight using living radical polymerization, which enables preparation of stimulus-responsive copolymer vesicles for the encapsulation and controlled release of active payloads.[25−40] In principle, disruption of vesicle membranes should be much more efficient than membrane swelling for the release of larger cargoes such as macromolecules or nanoparticles. In this context, there are various literature examples of vesicle dissociation to afford molecularly dissolved copolymer chains (a so-called *order−disorder* transition), whereby the membrane-forming hydrophobic block is rendered hydrophilic in situ.[41−47] In contrast, vesicle-to-worm or vesicle-to-sphere *order−order* transitions have been recently reported, which can also be used to trigger the on-demand release of encapsulated nanoparticle cargoes.[48−51] These latter transitions are typically the result of a subtle reduction in the geometric packing parameter[52] arising from the responsive behavior of either the stabilizer block or the membrane-forming block toward an external stimulus such as temperature,[53−57] pH,[58−61] CO_2,[62] cross-linker,[63] enzyme,[64] or redox.[65] In principle, vesicles that undergo morphological transitions after selectively binding to specific analytes (either by covalent bond formation or by host−guest supermolecular interactions) present in the external solution offer new strategies for targeted delivery and release applications.[49,50,66,67] In this context, dynamic covalent chemistry, which can be both highly selective and reversible, has been exploited by various research groups for the design of stimulus-responsive polymers utilizing acylhydrazone bonds,[68] imine bonds,[69] Diels−Alder chemistry,[70] Se−N bonds,[71] etc.[72−78] In particular, the reversible binding of phenylboronic acids with cis-diols has recently become the subject of considerable attention,[79−83] not least because of various potential biomedical applications involving detection of glucose, local pH, and adenosine

Received: March 16, 2017
Published: May 12, 2017

DOI: 10.1021/jacs.7b02642
J. Am. Chem. Soc. 2017, 139, 7616−7623

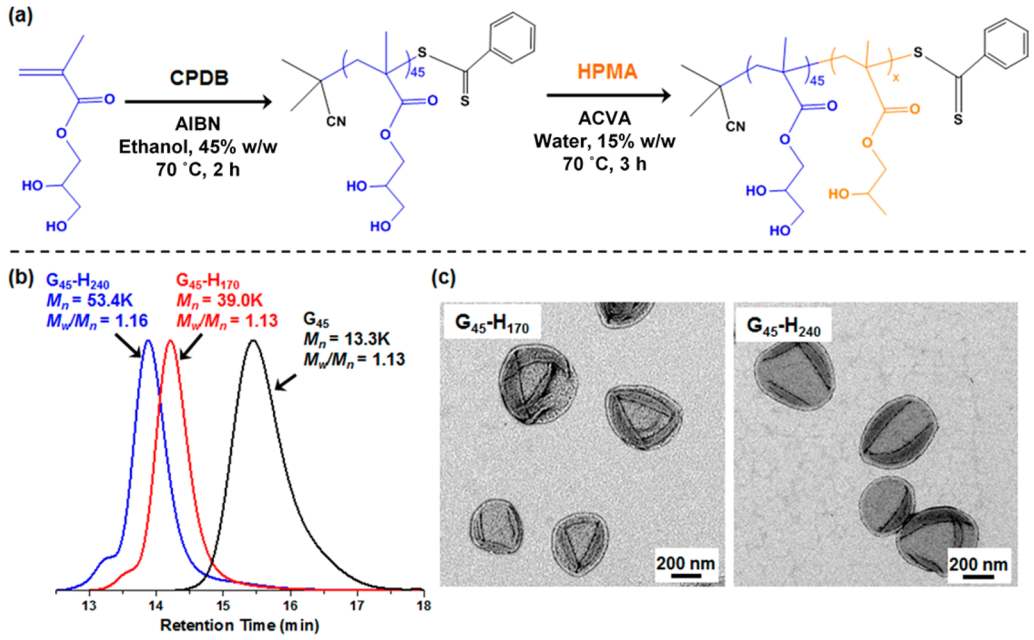

Figure 1. (a) Synthesis of $PGMA_{45}$ macro-CTA via RAFT solution polymerization of GMA and preparation of $PGMA_{45}$–$PHPMA_x$ diblock copolymer vesicles via RAFT aqueous dispersion polymerization of HPMA. (b) DMF GPC curves recorded for the $PGMA_{45}$ macro-CTA (black curve) and the corresponding $PGMA_{45}$–$PHPMA_{170}$ (red curve) and $PGMA_{45}$–$PHPMA_{240}$ (blue curve) diblock copolymers. (c) Representative TEM images obtained for the $PGMA_{45}$–$PHPMA_{170}$ and $PGMA_{45}$–$PHPMA_{240}$ vesicles, respectively.

triphosphate.[43,81,84−90] However, as far as we are aware, the use of such dynamic covalent chemistry to induce order−order morphological transitions in aqueous copolymer vesicles using water-soluble phenylboronic acid derivatives has not yet been reported in the literature.

In the present study, we introduce a new concept: dynamic covalent chemistry is utilized to drive order−order morphological transitions in aqueous dispersions of diblock copolymer vesicles in order to release nanoparticle payloads (and also to induce sol−gel transitions). More specifically, we use polymerization-induced self-assembly (PISA)[91−93] to prepare poly(glycerol monomethacrylate)−poly(2-hydroxypropyl methacrylate) (PGMA−PHPMA) diblock copolymer vesicles in concentrated aqueous solution.[94−97] This particular diblock copolymer was selected because (i) the PGMA block contains pendent cis-diol groups that can bind selectively to water-soluble phenylboronic acid derivatives[98] and (ii) the PHPMA block is only weakly hydrophobic, which facilitates the desired order−order morphological transition. Moreover, if such PGMA−PHPMA vesicles are prepared in the presence of an ultrafine aqueous silica sol or a globular protein, then a significant fraction of these nanoparticles can be encapsulated and thus serve as a model cargo.[48] Mable and co-workers recently reported that silica nanoparticle release can be achieved by cooling such PGMA−PHPMA vesicles from 20 °C to around 0 °C because this induces a vesicle-to-sphere transition.[48] However, a thermal trigger operating at sub-ambient temperature is unlikely to be desirable for many commercial applications. Furthermore, PGMA−PHPMA vesicles comprising relatively long PHPMA blocks (i.e., thicker-walled vesicles) simply do not undergo thermally induced morphological transitions.[59,60] Herein, we demonstrate that dynamic covalent chemistry can drive morphological transitions for PGMA−PHPMA vesicles in the presence of 3-aminophenylboronic acid (APBA) at ambient temperature and in the presence of salt, *even for vesicle-forming copolymer compositions that do not normally exhibit thermoresponsive behavior*. This versatile molecular recognition approach enables excellent control to be achieved over the rate of release of encapsulated nanoparticles simply by varying the pH and/or APBA concentration.

RESULTS AND DISCUSSION

A $PGMA_{45}$ macromolecular chain transfer agent (macro-CTA; the subscript refers to its mean degree of polymerization, DP) was synthesized by reversible addition−fragmentation chain transfer (RAFT) solution polymerization of glycerol monomethacrylate (GMA) in ethanol using a 2-cyano-2-propyl dithiobenzoate (CPDB) chain transfer agent (CTA) and 2,2′-azobis(isobutyronitrile) (AIBN) initiator (see Figure 1a). This water-soluble macro-CTA was then chain-extended via RAFT aqueous dispersion polymerization of 2-hydroxypropyl methacrylate (HPMA) initiated by 4,4′-azobis(4-cyanopentanoic acid) (ACVA) to produce well-defined $PGMA_{45}$–$PHPMA_x$ diblock copolymer vesicles at 15% w/w solids. A mean DP of either 170 or 240 was targeted for the membrane-forming PHPMA block. The lower DP corresponds to *thermosensitive* vesicles, whereas the higher DP corresponds to *thermostable* vesicles.[59,60] Gel permeation chromatography (GPC; DMF eluent) analyses indicated relatively narrow molecular weight distributions ($M_w/M_n \leq 1.16$) for the $PGMA_{45}$ macro-CTA precursor and both $PGMA_{45}$–$PHPMA_x$ diblock copolymers, as well as high blocking efficiencies (see Figure 1b). Well-defined pure vesicular morphologies were confirmed by transmission electron microscopy (TEM) studies (see Figure 1c).

APBA was added to a 0.20% w/w aqueous dispersion of $PGMA_{45}$–$PHPMA_{170}$ vesicles (molar concentration of GMA [G] repeat units = 2.9 mM) at an initial pH of 10.5 (a slight reduction in pH was observed after phenylboronate ester formation[99]). In the presence of 5.8 mM APBA, which corresponds to a APBA/GMA (or [B]/[G]) molar ratio of 2.0, all of the original vesicles were transformed into either

DOI: 10.1021/jacs.7b02642
J. Am. Chem. Soc. 2017, 139, 7616−7623

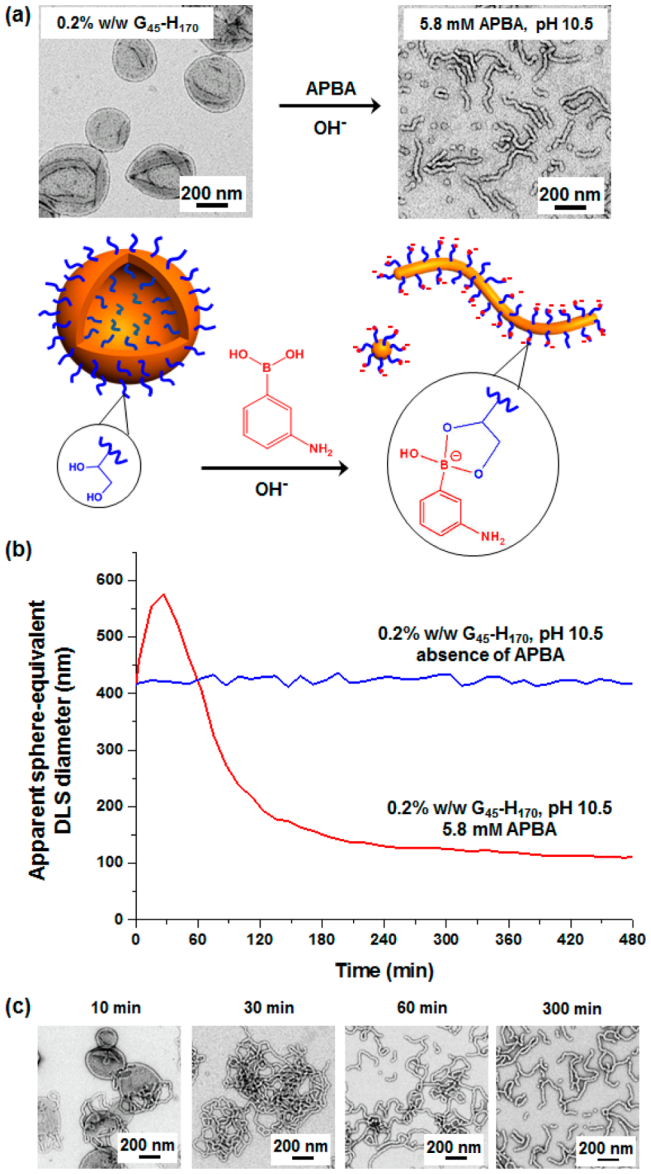

Figure 2. (a) TEM images obtained for an aqueous dispersion of 0.20% w/w $PGMA_{45}$–$PHPMA_{170}$ vesicles before and after APBA addition at pH 10.5 and the corresponding schematic cartoon depicting the vesicle-to-worm (or vesicle-to-sphere) transition that occurs after selective binding of APBA to the PGMA stabilizer chains. (b) Evolution in the apparent sphere-equivalent DLS diameter for a 0.20% w/w aqueous dispersion of $PGMA_{45}$–$PHPMA_{170}$ nano-objects recorded over time in the presence of 5.8 mM APBA at an initial pH of 10.5 (red curve) and (c) corresponding TEM images indicating the various changes in copolymer morphology observed during this kinetic experiment. The blue curve shown in (b) is the control experiment conducted in the absence of APBA at the same pH.

worms or spheres after aging for 15 h according to TEM studies (see Figure 2a). In contrast, the same vesicles undergo no change in morphology when aged for the same time at pH 10.5 in the absence of APBA (see Figure S2a in the Supporting Information). The aqueous vesicle dispersion was originally prepared at pH 5.8, so this control experiment confirms that alkalinity alone is not sufficient to induce an order-order transition. The observed changes in copolymer morphology occur because the APBA selectively binds to the PGMA chains via formation of phenylboronate ester bonds (see schematic cartoon in Figure 2a). This complexation increases the effective volume fraction of this stabilizer block by both increasing its effective mass and also introducing anionic charge,[100] which in turn reduces the geometric packing parameter for the copolymer chains.[52]

The gradual morphological evolution that occurs in the presence of APBA was monitored over 8 h using dynamic light scattering (DLS); see Figure 2b. Initially, the sphere-equivalent hydrodynamic particle diameter *increased* relative to the original vesicle diameter. This indicates the formation of either jellyfish or branched worms, as observed by TEM (see Figure 2c). The subsequent reduction in apparent particle diameter indicates the formation of worms and/or spheres, which is also confirmed by TEM studies (see Figure 2c). The change in copolymer morphology can be tuned by varying the APBA concentration because this affects its extent of binding with the PGMA chains. For example, using 2.9 mM APBA produced only branched worms after aging for 15 h, whereas using 14.5 mM APBA yielded a mixture of mainly spheres plus a few short worms from an initial 0.20% aqueous dispersion of $PGMA_{45}$–$PHPMA_{170}$ vesicles under otherwise identical conditions, as judged by TEM and DLS studies (see Figure S2).

When a 10% w/w aqueous dispersion of $PGMA_{45}$–$PHPMA_{170}$ vesicles ([G] = 145 mM) was examined, the addition of 7.25 mM APBA at pH 10.5 ([B]/[G] = 0.05) induced macroscopic gelation (see insets shown in Figure S3a), which implies a vesicle-to-worm transition.[101] Rheological studies indicated an increase in the storage modulus (G') up to a plateau value of approximately 76 Pa occurred within 70 min (see Figure S3a). In contrast, addition of 14.5 mM APBA ([B]/[G] = 0.10) to the same vesicle dispersion led to *initial* formation of a free-standing gel, but subsequent degelation produced a free-flowing dispersion of relatively low turbidity (see Figure S3b). These observations suggest that an initial vesicle-to-worm transition is followed by a worm-to-sphere transition. This interpretation is consistent with the local maximum in G' obtained in rheological studies of the same vesicle dispersion after APBA addition (see Figure S3b).

Small-angle X-ray scattering (SAXS) was utilized for in situ studies of the vesicle-to-worm-to-sphere transition (and concomitant sol–gel–sol transition[102]) exhibited by a 10% w/w aqueous dispersion of $PGMA_{45}$–$PHPMA_{170}$ vesicles after addition of 14.5 mM APBA at pH 10.5 (see Figure 3). The initial SAXS pattern exhibits an approximate −2 gradient at low q, which confirms that the original copolymer morphology corresponds to vesicles.[103] Morphological assignments were made at various time intervals after APBA addition by monitoring the gradient of the SAXS pattern in the low q regime ($0.06\ nm^{-1} < q < 0.10\ nm^{-1}$). Soon after APBA addition, this gradient became shallower, indicating the onset of a change in morphology. Informed by the above TEM studies, the original vesicles are most likely initially transformed into a mixed phase comprising vesicles, jellyfish, and worms. Since anisotropic worms exhibit a low q gradient of approximately −1,[103] the highest proportion of worms is obtained after ∼10 min (see Figure 3 inset, blue squares). This interpretation is consistent with complementary time-dependent rheological studies performed on the same 10% w/w aqueous vesicle dispersion (see Figure S3b), whereby the maximum G' value (corresponding to a free-standing gel) was obtained 10 min after APBA addition. The low q gradient continued to become shallower after this time point until a limiting value of around −0.35 was observed after ∼25 min, which is indicative of

DOI: 10.1021/jacs.7b02642
J. Am. Chem. Soc. 2017, 139, 7616–7623

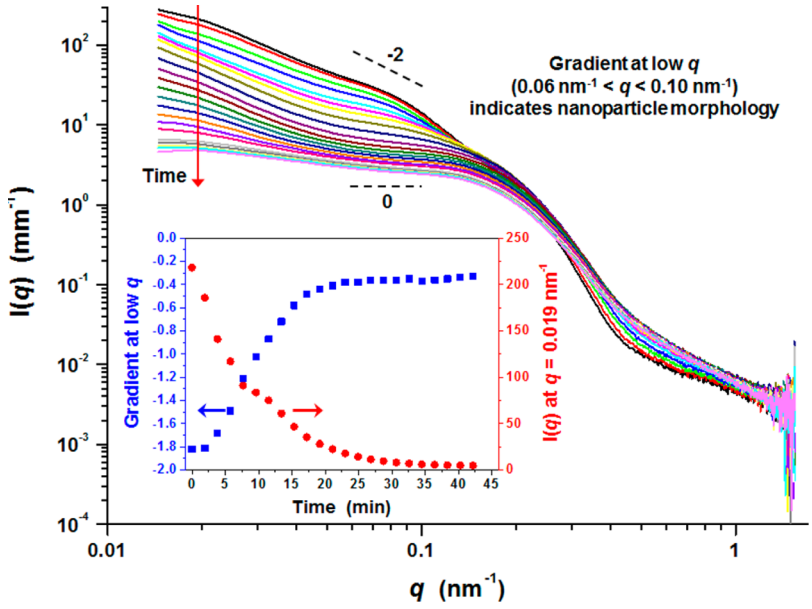

Figure 3. SAXS patterns recorded for a 10% w/w aqueous dispersion of $PGMA_{45}$–$PHPMA_{170}$ nano-objects at pH 10.5 after APBA addition. Representative lines with gradients of −2 and zero are shown as a guide to the eye. Inset: Evolution in (i) the gradient of the SAXS patterns in the low q regime [0.06 nm^{-1} < q < 0.10 nm^{-1}] (blue squares) and (ii) the X-ray scattering intensity at q = 0.019 nm^{-1} [as indicated by the vertical red arrow] (red circles) over time after APBA addition.

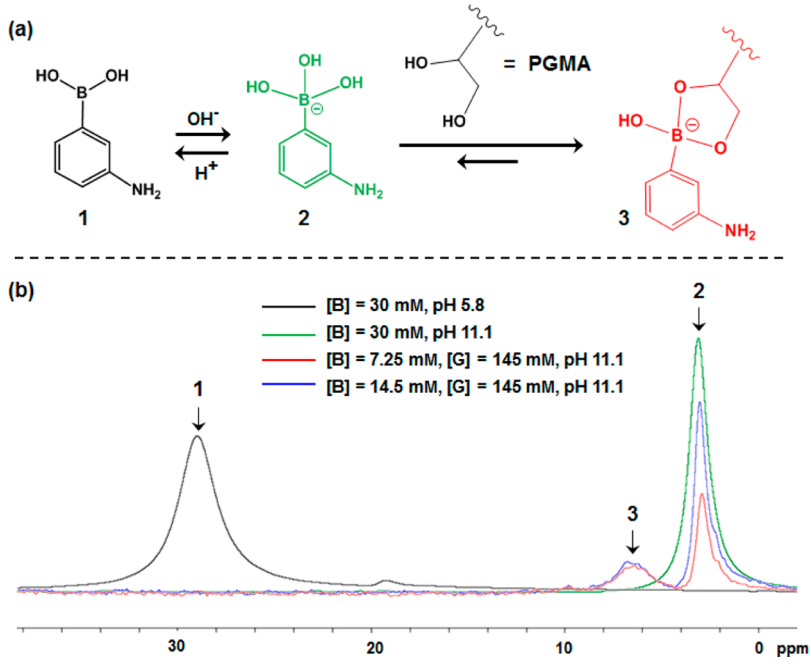

Figure 4. (a) Reaction scheme for APBA binding to PGMA in mildly alkaline solution. (b) Corresponding ^{11}B NMR spectra recorded for aqueous solutions containing 30 mM APBA at either pH 5.8 (black spectrum) or pH 11.1 (green spectrum) and binary mixtures of $PGMA_{45}$ ([G] = 145 mM) and APBA at pH 11.1 (red and blue spectra).

weakly aggregated spherical nano-objects. Monitoring the X-ray scattering intensity at q = 0.019 nm^{-1} provides a crude indication of the nano-object dimensions at any given time (see Figure 3 inset, red circles). This intensity is rapidly reduced from an initial value of ~220 mm^{-1} to a limiting value of ~5 mm^{-1} within ~35 min, which suggests that the original vesicles are converted into much smaller nano-objects. Such observations are in good agreement with oscillatory rheology data, which confirm that the intermediate gel is converted into a free-flowing fluid after ~35 min. This macroscopic degelation suggests that the dispersion consists mainly of spheres at this time point.

APBA binding to the PGMA chains was investigated using ^{11}B NMR spectroscopy.[104] It is well-known that (i) a pH-dependent equilibrium exists between phenylboronic acid (and its derivatives, as in this study) and phenylboronate ion[105] and (ii) the latter species can bind with cis-diol groups to form a phenylboronate ester (see Figure 4a). ^{11}B NMR spectra (see Figure 4b) confirmed a high degree of APBA ionization when increasing the solution pH from 5.8 to 11.1. The original ^{11}B

DOI: 10.1021/jacs.7b02642
J. Am. Chem. Soc. 2017, 139, 7616−7623

NMR signal recorded at approximately 29 ppm for APBA at pH 5.8 (black spectrum) shifts to 3.3 ppm after ionization at pH 11.1 (green spectrum). A new ^{11}B signal appears at 6.8 ppm in the presence of 7.25 mM $PGMA_{45}$ ([B]/[G] = 0.05), which indicates phenylboronate ester formation at pH 11.1 (red spectrum). On the basis of these ^{11}B NMR studies, we estimate that ~38% of the APBA binds to the GMA residues, which corresponds to approximately 0.8 APBA binding events per $PGMA_{45}$ chain, as calculated using eq 1.

$$n = f \times \frac{[B]}{[G]} \times DP_G \quad (1)$$

where n is the number of APBA molecules bound per $PGMA_{45}$ chain, f is the fraction of bound APBA (e.g., 38%), and DP_G is the mean DP of the PGMA chains (45). Increasing APBA to 14.5 mM leads to a lower bound fraction f of 0.24 (blue spectrum), which is attributed to the higher [B]/[G] molar ratio of 0.1. In this case, there are around 1.1 phenylboronate ester bonds per $PGMA_{45}$ chain. Approximately one phenylboronate ester (and hence one anionic charge) per stabilizer block is clearly sufficient to induce a vesicle-to-worm or vesicle-to-sphere transition (see Figures S3 and 3). It is noteworthy that this is comparable to the end-group ionization/protonation effect previously reported by Armes and co-workers.[59,60] More specifically, it was found that the ionization of a single carboxylic acid group located at the end of the PGMA stabilizer chain can confer pH-responsive character on $PGMA_{43}$–$PHPMA_{175}$ vesicles.[59] However, no morphological transition could be induced in the presence of 100 mM KCl for such vesicles. This is a significant disadvantage for potential commercial applications because many industrial formulations (e.g., liquid laundry products) contain salt. Thus, in the present study, we examined whether $PGMA_{45}$–$PHPMA_{170}$ vesicles could exhibit a morphological transition in the presence of both APBA and 100 mM NaCl. A 0.20% w/w aqueous dispersion of vesicles was converted into highly branched worms but only when using a [B]/[G] molar ratio of 2.0 (see Figure S4a). This suggests that the added salt either suppresses APBA binding to the PGMA stabilizer chains or partially screens the resulting anionic charge. Nevertheless, increasing the APBA concentration ([B] = 14.5 mM) to target a [B]/[G] molar ratio of 5.0 enabled both vesicle-to-worm and vesicle-to-sphere transformations to be achieved, even in the presence of 100 mM salt (see Figure S4b). In addition, such morphological transitions can occur in the presence of buffer, as shown in Figure S4c.

The effect of adding APBA to thicker-walled vesicles prepared using relatively long membrane-forming PHPMA blocks was also investigated. In control experiments, no morphological transition was observed for $PGMA_{45}$–$PHPMA_{240}$ vesicles after cooling to 2 °C for 20 h at either pH 5.8 or 10.5 (see Figure S5a,b). In striking contrast, a vesicle-to-worm transition could be induced for such $PGMA_{45}$–$PHPMA_{240}$ vesicles using our dynamic covalent chemistry strategy when selecting a [B]/[G] molar ratio of 5.0 ([B] = 11.1 mM) at pH 10.5 (see Figure S5d), whereas no transition occurred when [B] = 2.2 mM (see Figure S5c). Increasing the [B]/[G] molar ratio enhances the extent of APBA binding to each PGMA block. When the PHPMA DP (or x value) was increased up to 300, no morphological transition was observed even at a [B]/[G] molar ratio of 10 (see Figure S6). Greater APBA binding to the PGMA stabilizer chains is required for the dissociation of thicker-walled $PGMA_{45}$–$PHPMA_x$ vesicles because they lie further from the vesicle/worm boundary. For [B]/[G] = 50 ([B] = 97.5 mM), branched worms were observed after aging for 20 h, which then slowly transformed into a mixture of worms and spheres after 96 h (see Figure S6).

Unlike our earlier report utilizing a thermally triggered transition for $PGMA_{58}$–$PHPMA_{250}$ vesicles at 0–5 °C,[48] APBA-induced vesicle dissociation enables encapsulated silica nanoparticles to be released at *ambient* temperature. Moreover, the rate of nanoparticle release can be fine-tuned by systematically varying the solution conditions. In this series of experiments, the solution pH was adjusted using ammonia rather than NaOH to avoid possible dissolution of the silica nanoparticles. We also chose to use precisely the same $PGMA_{58}$–$PHPMA_{250}$ vesicles as those reported in ref 48 to facilitate a direct comparison. First, these vesicles were prepared via PISA in the *absence* of silica nanoparticles and studied by TEM and DLS to establish the conditions required for the vesicle-to-worm (or vesicle-to-sphere) transition (see Figure S7). The morphological transformation exhibited by $PGMA_{58}$–$PHPMA_{250}$ vesicles in the presence of APBA is subtly different from that observed for $PGMA_{45}$–$PHPMA_{240}$ vesicles under the same conditions. The longer PGMA stabilizer block means that the former vesicles lie closer to the vesicle/worm boundary. Thus, unlike the $PGMA_{45}$–$PHPMA_{240}$ vesicles, the $PGMA_{58}$–$PHPMA_{250}$ vesicles are thermoresponsive and undergo dissociation on cooling to 0–5 °C,[48] even though they possess thicker vesicle membranes. Furthermore, more APBA molecules can be bound to each (longer) PGMA chain.

For silica-loaded $PGMA_{58}$–$PHPMA_{250}$ vesicles, the encapsulated silica nanoparticles were fully released after 12 h at 20 °C in the presence of 12.6 mM APBA ([B]/[G] = 5.0) at an initial pH of 10.5 because these conditions led to the transformation of the vesicles into either worms or spheres (see Figure 5a). DLS studies confirmed a secondary population at around 20 nm (see Figure 5b). This feature is assigned to the released silica nanoparticles because no such population was observed in the control experiment conducted in the absence of any silica (see Figure S7b). It is only a minor population because the copolymer nano-objects (apparent sphere-equivalent diameter = 75 nm) scatter light much more strongly than the relatively small silica nanoparticles.

The rate of vesicle dissociation, and hence the rate of release of the silica nanoparticles, can be conveniently monitored by examining the dispersion turbidity over time. The original vesicles form a highly turbid dispersion, which becomes much less opaque as a result of the vesicle-to-worm (or vesicle-to-sphere) transition; see the inset digital photographs in Figure 5b. Thus, the absorbance of a 0.20% w/w aqueous dispersion of silica-loaded $PGMA_{58}$–$PHPMA_{250}$ vesicles in the presence of 12.6 mM APBA at pH 10.5 was monitored at a fixed wavelength of 450 nm over a 15 h period at ambient temperature (~20 °C), see Figure 6 (black curve). An approximately linear reduction in absorbance was observed within the first 7 h, with a relatively constant final value of around 0.12 being observed after 12 h. According to the reaction equilibria shown in Figure 4a, phenylboronate anions are formed at higher pH and this species binds strongly to the PGMA chains. In practice, this means that the release rate of the silica nanoparticles can be readily controlled by varying either the APBA concentration or the solution pH. Thus, doubling the APBA concentration to 25.2 mM leads to a much more rapid reduction in turbidity, which is almost complete within 2 h (see blue curve). In contrast, essentially no change in

DOI: 10.1021/jacs.7b02642
J. Am. Chem. Soc. 2017, 139, 7616–7623

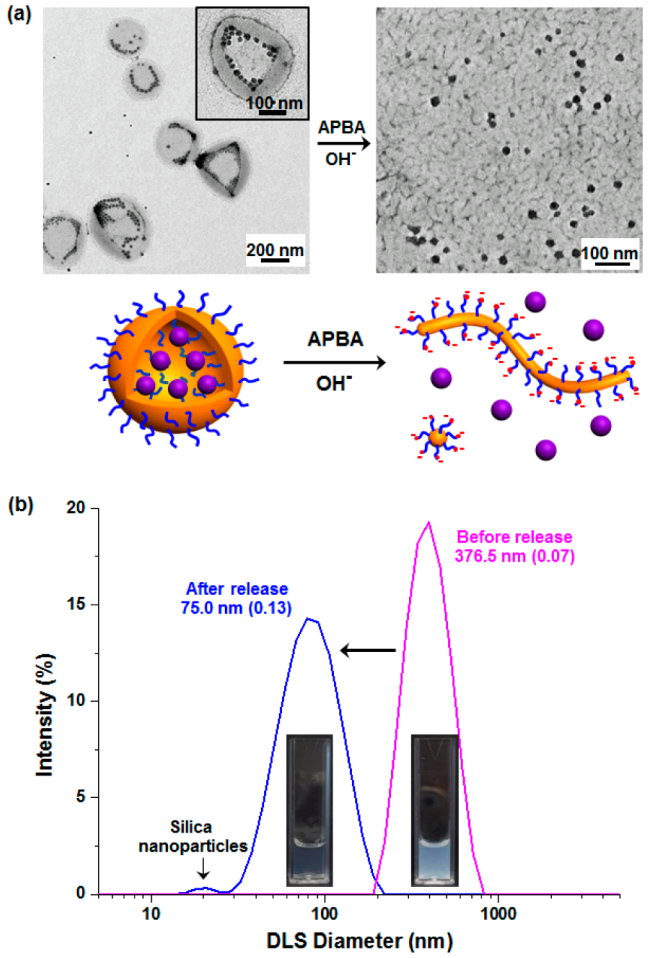

Figure 5. (a) Representative TEM images and (b) DLS particle size distribution curves demonstrating that dissociation of 0.20% w/w $PGMA_{58}$–$PHPMA_{250}$ vesicles loaded with 8.0% silica nanoparticles at an initial pH of 10.5 in the presence of 12.6 mM APBA leads to release of the encapsulated silica nanoparticles.

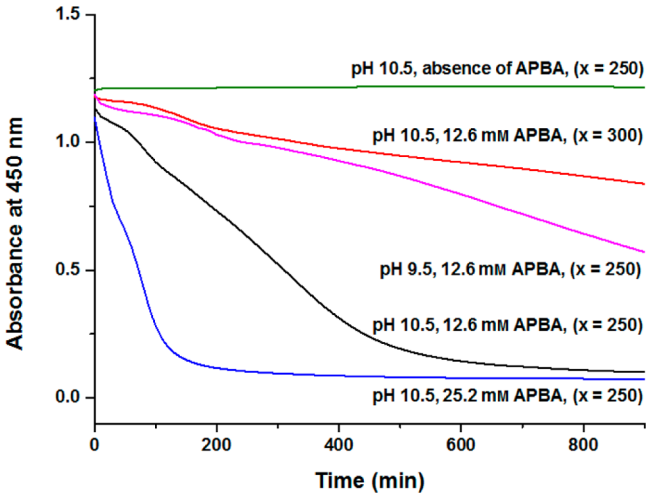

Figure 6. Absorbance vs time curves recorded at a fixed wavelength of 450 nm for a 0.20% w/w aqueous dispersion of silica-loaded $PGMA_{58}$–$PHPMA_x$ vesicles when subjected to various release conditions (see labeled curves for details; *x* refers to the mean degree of polymerization of the weakly hydrophobic membrane-forming PHPMA block).

turbidity was observed in the absence of any APBA (see green curve). Lowering the solution pH by one unit (from pH 10.5 to 9.5) significantly retards the rate of nanoparticle release (compare the pink and black curves). Finally, increasing the DP of the membrane-forming PHPMA block from 250 to 300 also leads to a much slower morphological transition under otherwise identical conditions (compare the red and black curves). Thus the vesicle membrane thickness is also an important parameter in determining the rate of silica nanoparticle release in the presence of APBA. Although the vesicles reported herein are somewhat polydisperse in terms of their overall diameter, they have relatively well-defined vesicle membranes. Hence the rate of nanoparticle release is essentially independent of vesicle size, although larger vesicles will, on average, contain more silica nanoparticles than smaller vesicles.

The encapsulation and release of silica nanoparticles from vesicles under the mildly alkaline conditions described herein is a useful model system for understanding the encapsulation of enzymes in concentrated liquid laundry products. In this case, it is essential to ensure that bleaching agents (e.g., H_2O_2) do not cause premature denaturation of enzymes such as protease, cellulose, lipase, or amylase during long-term storage. In principle, enzyme encapsulation within vesicles at 40 °C can prevent this bleach deactivation problem,[48] with subsequent APBA binding during the laundry wash at pH 9–10 leading to in situ release of the enzymes. If alternative applications are desired, the alkaline pH required for APBA binding to the PGMA stabilizer chains can be lowered by selecting phenylboronic acid derivatives with appropriate substituents. For example, electron-withdrawing nitro groups can lower the effective pK_a to 7.1.[106] Similarly, intramolecular coordination between the electron-deficient boron and an electron-rich ortho group, e.g., *o*-hydroxymethyl phenylboronic acid (pK_a ~ 7.2),[107] enables binding to occur at physiological pH rather than pH 9–10.

CONCLUSIONS

In summary, specific binding of APBA to the pendent cis-diol groups on PGMA stabilizer chains in mildly alkaline media can be used to drive morphological transitions for PGMA–PHPMA diblock copolymer vesicles. This dynamic covalent chemistry strategy can provide remarkably good control over the rate of release of encapsulated silica nanoparticles. Moreover, unlike earlier vesicle dissociation mechanisms based on the thermoresponsive nature of the membrane-forming PHPMA block or the ionization (or protonation) of functional groups located on the stabilizer terminus, this approach works well at ambient temperature, in the presence of relatively high levels of added salt, and even for thick-walled vesicles that do not normally exhibit thermosensitivity. In principle, this dynamic covalent chemistry strategy can be extended to include other block copolymers and perhaps also other types of vesicles such as liposomes. In summary, the combination of molecular recognition with appropriately designed block copolymer vesicles appears to offer considerable scope for targeted delivery and controlled release applications.

ASSOCIATED CONTENT

Supporting Information

The Supporting Information is available free of charge on the ACS Publications website at DOI: 10.1021/jacs.7b02642.

DOI: 10.1021/jacs.7b02642
J. Am. Chem. Soc. 2017, 139, 7616–7623

Experimental section; ^{1}H NMR spectrum of $PGMA_{45}$ macro-CTA; additional TEM images and DLS data for $PGMA_{45}$–$PHPMA_{170}$ nano-objects in the presence/absence of salt; rheology traces of the morphological transitions of 10% w/w $PGMA_{45}$–$PHPMA_{170}$; TEM images and DLS data of vesicles before and after transitions for $PGMA_{45}$–$PHPMA_{240}$, $PGMA_{45}$–$PHPMA_{300}$, and $PGMA_{58}$–$PHPMA_{250}$ (PDF)

AUTHOR INFORMATION

Corresponding Authors

*rhd.deng@gmail.com (R.D.)
*s.p.armes@sheffield.ac.uk (S.P.A.)

ORCID

Renhua Deng: 0000-0001-7217-5772
Matthew J. Derry: 0000-0001-5010-6725
Steven P. Armes: 0000-0002-8289-6351

Notes

The authors declare no competing financial interest.

ACKNOWLEDGMENTS

We thank the European Research Council for a five-year Advanced Investigator grant (PISA 320372). EPSRC is also thanked for partial funding of this work (EP/J007846/1). We are grateful to the European Synchrotron Radiation Facility (ESRF, Grenoble, France) for providing synchrotron beam-time and thank Dr. R. Dattani and the personnel of the ID02 station for their technical assistance.

REFERENCES

(1) Bellomo, E. G.; Wyrsta, M. D.; Pakstis, L.; Pochan, D. J.; Deming, T. J. *Nat. Mater.* **2004**, *3*, 244.
(2) Mura, S.; Nicolas, J.; Couvreur, P. *Nat. Mater.* **2013**, *12*, 991.
(3) Antonietti, M.; Förster, S. *Adv. Mater.* **2003**, *15*, 1323.
(4) Versluis, F.; Tomatsu, I.; Kehr, S.; Fregonese, C.; Tepper, A. W. J. W.; Stuart, M. C. A.; Ravoo, B. J.; Koning, R. I.; Kros, A. *J. Am. Chem. Soc.* **2009**, *131*, 13186.
(5) Guo, D.-S.; Wang, K.; Wang, Y.-X.; Liu, Y. *J. Am. Chem. Soc.* **2012**, *134*, 10244.
(6) Yao, Y.; Xue, M.; Chen, J.; Zhang, M.; Huang, F. *J. Am. Chem. Soc.* **2012**, *134*, 15712.
(7) Duan, Q.; Cao, Y.; Li, Y.; Hu, X.; Xiao, T.; Lin, C.; Pan, Y.; Wang, L. *J. Am. Chem. Soc.* **2013**, *135*, 10542.
(8) Cao, Y.; Hu, X.-Y.; Li, Y.; Zou, X.; Xiong, S.; Lin, C.; Shen, Y.-Z.; Wang, L. *J. Am. Chem. Soc.* **2014**, *136*, 10762.
(9) Chen, L.-J.; Zhao, G.-Z.; Jiang, B.; Sun, B.; Wang, M.; Xu, L.; He, J.; Abliz, Z.; Tan, H.; Li, X.; Yang, H.-B. *J. Am. Chem. Soc.* **2014**, *136*, 5993.
(10) Guo, J.; Zhuang, J.; Wang, F.; Raghupathi, K. R.; Thayumanavan, S. *J. Am. Chem. Soc.* **2014**, *136*, 2220.
(11) Wu, X.; Busschaert, N.; Wells, N. J.; Jiang, Y.-B.; Gale, P. A. *J. Am. Chem. Soc.* **2015**, *137*, 1476.
(12) Chen, X.; He, Y.; Kim, Y.; Lee, M. *J. Am. Chem. Soc.* **2016**, *138*, 5773.
(13) Karimi, M.; Sahandi Zangabad, P.; Baghaee-Ravari, S.; Ghazadeh, M.; Mirshekari, H.; Hamblin, M. R. *J. Am. Chem. Soc.* **2017**, *139*, 4584.
(14) Tan, X.; Li, B. B.; Lu, X.; Jia, F.; Santori, C.; Menon, P.; Li, H.; Zhang, B.; Zhao, J. J.; Zhang, K. *J. Am. Chem. Soc.* **2015**, *137*, 6112.
(15) Gaitzsch, J.; Huang, X.; Voit, B. *Chem. Rev.* **2016**, *116*, 1053.
(16) Tanner, P.; Baumann, P.; Enea, R.; Onaca, O.; Palivan, C.; Meier, W. *Acc. Chem. Res.* **2011**, *44*, 1039.
(17) Chi, X.; Ji, X.; Xia, D.; Huang, F. *J. Am. Chem. Soc.* **2015**, *137*, 1440.
(18) Wong, C. K.; Laos, A. J.; Soeriyadi, A. H.; Wiedenmann, J.; Curmi, P. M. G.; Gooding, J. J.; Marquis, C. P.; Stenzel, M. H.; Thordarson, P. *Angew. Chem., Int. Ed.* **2015**, *54*, 5317.
(19) Jain, S.; Bates, F. S. *Science* **2003**, *300*, 460.
(20) Discher, D. E.; Eisenberg, A. *Science* **2002**, *297*, 967.
(21) Discher, B. M.; Won, Y.-Y.; Ege, D. S.; Lee, J. C.-M.; Bates, F. S.; Discher, D. E.; Hammer, D. A. *Science* **1999**, *284*, 1143.
(22) Kukula, H.; Schlaad, H.; Antonietti, M.; Förster, S. *J. Am. Chem. Soc.* **2002**, *124*, 1658.
(23) Battaglia, G.; Ryan, A. J. *J. Am. Chem. Soc.* **2005**, *127*, 8757.
(24) Du, J.; Tang, Y.; Lewis, A. L.; Armes, S. P. *J. Am. Chem. Soc.* **2005**, *127*, 17982.
(25) Hu, X.; Hu, J.; Tian, J.; Ge, Z.; Zhang, G.; Luo, K.; Liu, S. *J. Am. Chem. Soc.* **2013**, *135*, 17617.
(26) Yan, B.; Han, D.; Boissiere, O.; Ayotte, P.; Zhao, Y. *Soft Matter* **2013**, *9*, 2011.
(27) Krack, M.; Hohenberg, H.; Kornowski, A.; Lindner, P.; Weller, H.; Förster, S. *J. Am. Chem. Soc.* **2008**, *130*, 7315.
(28) Wilson, D. A.; Nolte, R. J. M.; van Hest, J. C. M. *J. Am. Chem. Soc.* **2012**, *134*, 9894.
(29) Peng, F.; Tu, Y.; van Hest, J. C. M.; Wilson, D. A. *Angew. Chem., Int. Ed.* **2015**, *54*, 11662.
(30) Zhu, Y.; Yang, B.; Chen, S.; Du, J. *Prog. Polym. Sci.* **2017**, *64*, 1.
(31) Ladmiral, V.; Semsarilar, M.; Canton, I.; Armes, S. P. *J. Am. Chem. Soc.* **2013**, *135*, 13574.
(32) van Rhee, P. G.; Rikken, R. S. M.; Abdelmohsen, L. K. E. A.; Maan, J. C.; Nolte, R. J. M.; van Hest, J. C. M.; Christianen, P. C. M.; Wilson, D. A. *Nat. Commun.* **2014**, *5*, 5010.
(33) Wang, L.; Chierico, L.; Little, D.; Patikarnmonthon, N.; Yang, Z.; Azzouz, M.; Madsen, J.; Armes, S. P.; Battaglia, G. *Angew. Chem., Int. Ed.* **2012**, *51*, 11122.
(34) Wilson, D. A.; Nolte, R. J. M.; van Hest, J. C. M. *Nat. Chem.* **2012**, *4*, 268.
(35) Rikken, R. S. M.; Engelkamp, H.; Nolte, R. J. M.; Maan, J. C.; van Hest, J. C. M.; Wilson, D. A.; Christianen, P. C. M. *Nat. Commun.* **2016**, *7*, 12606.
(36) Wang, X.; Hu, J.; Liu, G.; Tian, J.; Wang, H.; Gong, M.; Liu, S. *J. Am. Chem. Soc.* **2015**, *137*, 15262.
(37) Oliveira, H.; Pérez-Andrés, E.; Thevenot, J.; Sandre, O.; Berra, E.; Lecommandoux, S. *J. Controlled Release* **2013**, *169*, 165.
(38) Yan, Q.; Zhou, R.; Fu, C.; Zhang, H.; Yin, Y.; Yuan, J. *Angew. Chem., Int. Ed.* **2011**, *50*, 4923.
(39) Deng, Z.; Qian, Y.; Yu, Y.; Liu, G.; Hu, J.; Zhang, G.; Liu, S. *J. Am. Chem. Soc.* **2016**, *138*, 10452.
(40) Du, J.; O'Reilly, R. K. *Soft Matter* **2009**, *5*, 3544.
(41) Kim, H.; Kang, Y. J.; Jeong, E. S.; Kang, S.; Kim, K. T. *ACS Macro Lett.* **2012**, *1*, 1194.
(42) Liu, G.; Wang, X.; Hu, J.; Zhang, G.; Liu, S. *J. Am. Chem. Soc.* **2014**, *136*, 7492.
(43) Kim, H.; Kang, Y. J.; Kang, S.; Kim, K. T. *J. Am. Chem. Soc.* **2012**, *134*, 4030.
(44) Qin, S.; Geng, Y.; Discher, D. E.; Yang, S. *Adv. Mater.* **2006**, *18*, 2905.
(45) Rodríguez-Hernández, J.; Lecommandoux, S. *J. Am. Chem. Soc.* **2005**, *127*, 2026.
(46) Schatz, C.; Louguet, S.; Le Meins, J.-F.; Lecommandoux, S. *Angew. Chem., Int. Ed.* **2009**, *48*, 2572.
(47) Lomas, H.; Canton, I.; MacNeil, S.; Du, J.; Armes, S. P.; Ryan, A. J.; Lewis, A. L.; Battaglia, G. *Adv. Mater.* **2007**, *19*, 4238.
(48) Mable, C. J.; Gibson, R. R.; Prevost, S.; McKenzie, B. E.; Mykhaylyk, O. O.; Armes, S. P. *J. Am. Chem. Soc.* **2015**, *137*, 16098.
(49) Ji, X.; Wang, H.; Li, Y.; Xia, D.; Li, H.; Tang, G.; Sessler, J. L.; Huang, F. *Chem. Sci.* **2016**, *7*, 6006.
(50) Li, Y.; Liu, G.; Wang, X.; Hu, J.; Liu, S. *Angew. Chem., Int. Ed.* **2016**, *55*, 1760.
(51) Chen, Q.; Schönherr, H.; Vancso, G. J. *Small* **2010**, *6*, 2762.
(52) Israelachvili, J. N.; Mitchell, D. J.; Ninham, B. W. *J. Chem. Soc., Faraday Trans. 2* **1976**, *72*, 1525.

DOI: 10.1021/jacs.7b02642
J. Am. Chem. Soc. 2017, 139, 7616–7623

(53) Sundararaman, A.; Stephan, T.; Grubbs, R. B. *J. Am. Chem. Soc.* **2008**, *130*, 12264.
(54) Bhargava, P.; Tu, Y.; Zheng, J. X.; Xiong, H.; Quirk, R. P.; Cheng, S. Z. D. *J. Am. Chem. Soc.* **2007**, *129*, 1113.
(55) Moughton, A. O.; Patterson, J. P.; O'Reilly, R. K. *Chem. Commun.* **2011**, *47*, 355.
(56) LaRue, I.; Adam, M.; Pitsikalis, M.; Hadjichristidis, N.; Rubinstein, M.; Sheiko, S. S. *Macromolecules* **2006**, *39*, 309.
(57) Abbas, S.; Li, Z.; Hassan; Lodge, T. P. *Macromolecules* **2007**, *40*, 4048.
(58) Maiti, C.; Banerjee, R.; Maiti, S.; Dhara, D. *Langmuir* **2015**, *31*, 32.
(59) Lovett, J. R.; Warren, N. J.; Armes, S. P.; Smallridge, M. J.; Cracknell, R. B. *Macromolecules* **2016**, *49*, 1016.
(60) Penfold, N. J. W.; Lovett, J. R.; Verstraete, P.; Smets, J.; Armes, S. P. *Polym. Chem.* **2017**, *8*, 272.
(61) Lee, M.; Lee, S.-J.; Jiang, L.-H. *J. Am. Chem. Soc.* **2004**, *126*, 12724.
(62) Yan, Q.; Zhao, Y. *J. Am. Chem. Soc.* **2013**, *135*, 16300.
(63) van Oers, M. C. M.; Rutjes, F. P. J. T.; van Hest, J. C. M. *J. Am. Chem. Soc.* **2013**, *135*, 16308.
(64) Ku, T.-H.; Chien, M.-P.; Thompson, M. P.; Sinkovits, R. S.; Olson, N. H.; Baker, T. S.; Gianneschi, N. C. *J. Am. Chem. Soc.* **2011**, *133*, 8392.
(65) Kim, H.; Jeong, S.-M.; Park, J.-W. *J. Am. Chem. Soc.* **2011**, *133*, 5206.
(66) Molla, M. R.; Prasad, P.; Thayumanavan, S. *J. Am. Chem. Soc.* **2015**, *137*, 7286.
(67) Chi, X.; Zhang, H.; Vargas-Zúñiga, G. I.; Peters, G. M.; Sessler, J. L. *J. Am. Chem. Soc.* **2016**, *138*, 5829.
(68) Whitaker, D. E.; Mahon, C. S.; Fulton, D. A. *Angew. Chem., Int. Ed.* **2013**, *52*, 956.
(69) Gu, J.; Cheng, W.-P.; Liu, J.; Lo, S.-Y.; Smith, D.; Qu, X.; Yang, Z. *Biomacromolecules* **2008**, *9*, 255.
(70) Bapat, A. P.; Ray, J. G.; Savin, D. A.; Hoff, E. A.; Patton, D. L.; Sumerlin, B. S. *Polym. Chem.* **2012**, *3*, 3112.
(71) Yi, Y.; Xu, H.; Wang, L.; Cao, W.; Zhang, X. *Chem. - Eur. J.* **2013**, *19*, 9506.
(72) Jackson, A. W.; Fulton, D. A. *Polym. Chem.* **2013**, *4*, 31.
(73) Mahon, C. S.; Fulton, D. A. *Chem. Sci.* **2013**, *4*, 3661.
(74) Jin, Y.; Yu, C.; Denman, R. J.; Zhang, W. *Chem. Soc. Rev.* **2013**, *42*, 6634.
(75) Rowan, S. J.; Cantrill, S. J.; Cousins, G. R. L.; Sanders, J. K. M.; Stoddart, J. F. *Angew. Chem., Int. Ed.* **2002**, *41*, 898.
(76) Kim, J.; Baek, K.; Shetty, D.; Selvapalam, N.; Yun, G.; Kim, N. H.; Ko, Y. H.; Park, K. M.; Hwang, I.; Kim, K. *Angew. Chem., Int. Ed.* **2015**, *54*, 2693.
(77) Wojtecki, R. J.; Meador, M. A.; Rowan, S. J. *Nat. Mater.* **2011**, *10*, 14.
(78) Maeda, T.; Otsuka, H.; Takahara, A. *Prog. Polym. Sci.* **2009**, *34*, 581.
(79) Bapat, A. P.; Roy, D.; Ray, J. G.; Savin, D. A.; Sumerlin, B. S. *J. Am. Chem. Soc.* **2011**, *133*, 19832.
(80) Cash, J. J.; Kubo, T.; Bapat, A. P.; Sumerlin, B. S. *Macromolecules* **2015**, *48*, 2098.
(81) Li, Y.; Xiao, W.; Xiao, K.; Berti, L.; Luo, J.; Tseng, H. P.; Fung, G.; Lam, K. S. *Angew. Chem., Int. Ed.* **2012**, *51*, 2864.
(82) Zhang, D.; Thompson, K. L.; Pelton, R.; Armes, S. P. *Langmuir* **2010**, *26*, 17237.
(83) Cunningham, V. J.; Alswieleh, A. M.; Thompson, K. L.; Williams, M.; Leggett, G. J.; Armes, S. P.; Musa, O. M. *Macromolecules* **2014**, *47*, 5613.
(84) Kim, K. T.; Cornelissen, J. J. L. M.; Nolte, R. J. M.; van Hest, J. C. M. *Adv. Mater.* **2009**, *21*, 2787.
(85) Ma, R.; Shi, L. *Polym. Chem.* **2014**, *5*, 1503.
(86) Roy, D.; Cambre, J. N.; Sumerlin, B. S. *Chem. Commun.* **2009**, 2106.
(87) Brooks, W. L. A.; Sumerlin, B. S. *Chem. Rev.* **2016**, *116*, 1375.
(88) Wang, B.; Ma, R.; Liu, G.; Li, Y.; Liu, X.; An, Y.; Shi, L. *Langmuir* **2009**, *25*, 12522.
(89) Yang, H.; Ma, R.; Yue, J.; Li, C.; Liu, Y.; An, Y.; Shi, L. *Polym. Chem.* **2015**, *6*, 3837.
(90) Naito, M.; Ishii, T.; Matsumoto, A.; Miyata, K.; Miyahara, Y.; Kataoka, K. *Angew. Chem., Int. Ed.* **2012**, *51*, 10751.
(91) Gonzato, C.; Semsarilar, M.; Jones, E. R.; Li, F.; Krooshof, G. J. P.; Wyman, P.; Mykhaylyk, O. O.; Tuinier, R.; Armes, S. P. *J. Am. Chem. Soc.* **2014**, *136*, 11100.
(92) Warren, N. J.; Armes, S. P. *J. Am. Chem. Soc.* **2014**, *136*, 10174.
(93) Canning, S. L.; Smith, G. N.; Armes, S. P. *Macromolecules* **2016**, *49*, 1985.
(94) Li, Y.; Armes, S. P. *Angew. Chem., Int. Ed.* **2010**, *49*, 4042.
(95) Blanazs, A.; Ryan, A. J.; Armes, S. P. *Macromolecules* **2012**, *45*, 5099.
(96) Blanazs, A.; Madsen, J.; Battaglia, G.; Ryan, A. J.; Armes, S. P. *J. Am. Chem. Soc.* **2011**, *133*, 16581.
(97) Warren, N. J.; Mykhaylyk, O. O.; Ryan, A. J.; Williams, M.; Doussineau, T.; Dugourd, P.; Antoine, R.; Portale, G.; Armes, S. P. *J. Am. Chem. Soc.* **2015**, *137*, 1929.
(98) Actually, the PGMA chains comprise a statistical mixture of the 1,2-diol (92%) and 1,3-diol (8%) isomers. Moreover, we cannot rule out the possibility that preferential binding of APBA might occur via the minor fraction of 1,3-diol units.
(99) Ni, W.; Fang, H.; Springsteen, G.; Wang, B. *J. Org. Chem.* **2004**, *69*, 1999.
(100) Usually, APBA exists in its protonated cationic form in aqueous solution. However, at pH 10.5, this molecule exists in its neutral form. Thus, APBA binding confers only anionic charge (via the boron atom; see Figure 2) rather than zwitterionic charge.
(101) Lovett, J. R.; Warren, N. J.; Ratcliffe, L. P. D.; Kocik, M. K.; Armes, S. P. *Angew. Chem., Int. Ed.* **2015**, *54*, 1279.
(102) Goujon, A.; Mariani, G.; Lang, T.; Moulin, E.; Rawiso, M.; Buhler, E.; Giuseppone, N. *J. Am. Chem. Soc.* **2017**, *139*, 4923.
(103) Glatter, O.; Kratky, O. *Small-Angle X-ray Scattering*; Academic Press: London, 1982.
(104) Pezron, E.; Leibler, L.; Ricard, A.; Lafuma, F.; Audebert, R. *Macromolecules* **1989**, *22*, 1169.
(105) Matsumoto, A.; Ikeda, S.; Harada, A.; Kataoka, K. *Biomacromolecules* **2003**, *4*, 1410.
(106) Torssell, K.; McClendon, J. H.; Somers, G. F.; Hartiala, K.; Veige, S.; Diczfalusy, E. *Acta Chem. Scand.* **1958**, *12*, 1373.
(107) Dowlut, M.; Hall, D. G. *J. Am. Chem. Soc.* **2006**, *128*, 4226.

DOI: 10.1021/jacs.7b02642
J. Am. Chem. Soc. 2017, 139, 7616−7623